Turkish Journal of Electrical Engineering & Computer Sciences

http://journals.tubitak.gov.tr/elektrik/

Research Article

Turk J Elec Eng & Comp Sci
(2018) 26: 1103 – 1114

doi:10.3906/elk-1706-23

Optimal sizing hydrokinetic-photovoltaic system for electricity generation in a protected wildlife area of Ecuador

Juan LATA-GARCIA[1,2,*], Francisco JURADO-MELGUIZO[2], Higinio SANCHEZ-SAINZ[3], Christopher REYES-LOPEZ[1], Luis FERNÁNDEZ-RAMIREZ[3]

[1]Department of Electrical Engineering (GIPI – SMART-TECH), Salesian Polytechnic University, Guayaquil, Ecuador

[2]Department of Electrical Engineering, University of Jaen, Linares, Spain

[3]Department of Electrical Engineering, University of Cadiz, Cadiz, Spain

Received: 02.06.2017 • **Accepted/Published Online:** 11.01.2018 • **Final Version:** 30.03.2018

Abstract: Rural electrification is one of the most significant issues faced by electricity companies. For this reason, these companies are choosing alternative sources to generate energy in isolated regions. Furthermore, hybrid generation systems are an effective option for supplying protected areas. In this context, this research aims at designing an autonomous hybrid system to meet the annual electricity demand of the inhabitants of a national park. Fluvial and solar energies are the best options to reduce environmental impact and to ensure the conservation of the endemic fauna and flora of the island at a low carbon footprint. The system comprises a series of subsystems modeled using commercial software for sizing and optimization. The main generation subsystem contains a hydrokinetic turbine and photovoltaic panels, the storage subsystem contains a battery bank, and the backup subsystem consists of a diesel generator used in case of lack of energy from the rest of suppliers of the hybrid system. The main results of the simulation show an optimized system that fulfills the energy demand while minimizing the use of the diesel generator to 5668 kWh/year (14.3%) of thorough generation. The hydrokinetic generator supplies 20,330 kWh/year (51.4% of the total generation) and the solar generator supplies 13,580 kWh/year (34.3%).

Key words: Fluvial turbines, hybrid generation, national park, photovoltaic panels, renewable energy

1. Introduction

Nowadays, nearly 1.4 billion people worldwide do not have access to electricity; almost 85% of them reside in rural areas [1]. In remote areas, such as islands, mountains, and deserts, electricity is usually supplied by generators based on internal combustion engines (ICEs). In most cases, the generation of energy from fossil fuels is considerably expensive and emits a significant amount of carbon dioxide (CO_2) into the air. Moreover, when using fossil fuels for electricity conversion in ICEs, most of their chemical energy is wasted in the form of thermal losses; hence, it converts a relatively small amount of energy into electricity [2]. In addition, the transport of such fuels to remote areas and its subsequent storage present several challenges.

Rural areas that lack mountainous landscapes make building hydroelectric dams impossible. However, these areas could be located in close proximity to rivers, with a significant water flow, which would allow leveraging the stream to generate energy. Moreover, this type of technology causes a lower environmental impact, making it attractive for small-scale usage, unlike a conventional electric system [3,4]. The suitable

*Correspondence: jlatag@ups.edu.ec

utilization of natural resources for a reliable energy supply is a very complex task due to diverse constraints, such as the absence of weather predictability.

A hybrid renewable energy (HRE) system consisting of solar and fluvial resources offers advantageous solutions for remote locations or areas not served by the national electric network [5].

The project carried out by Montoya et al. shows a valuable technological approach considering the kinetic energy of discharge channels of large hydroelectric power stations [6]. It presents a good start to support the functionality of the subsystem working with the river flow and compliance with the energy levels required to generate.

According to numerous studies, hybrid systems are more reliable for sizing than those using only one type of renewable generation [7]. This is the reason several authors apply assorted methods and algorithms for better optimization [8].

An appropriate sizing of a hybrid system, including the development of mathematical models and the adoption of optimization techniques, is required to achieve a technologically and economically efficient exploitation of the resources. In this context, the hybrid optimization model for renewable electricity (HOMER) software is a powerful tool to solve sizing issues through the use of environmental data load per hour, optimally minimizing the cost of the system net present value [9].

Another powerful tool for the optimal technical sizing of hybrid renewable energy generation systems [8] is the Simulink Design Optimization (SDO) by MATLAB, which will be used for the development of this project.

2. Background

The hybrid generation system model proposed in this paper is designed to meet the energy demand of the inhabitants of Santay Island in Ecuador. Thus, it will comply with the Ecuadorian Plan of Electrification and support the Ecuadorian strategy to achieve energy sustainability [10]. Santay is a small landmass located in the Gulf of Guayaquil, only 800 m away from the city of Guayaquil, with an area of 21.79 km^2. It houses a population of 235 persons divided among 56 families living in 46 houses, most of them at the entrance of this natural park. Figure 1 is an aerial view of the island.

Various studies carried out abroad employ tools to model the system and to perform the optimization

Figure 1. Panoramic view of Santay Island. Source: Guayaquil Company of Tourism, Civic Promotion and International Relations.

procedure of this research. For instance, Ahmadi et al. propose a hybrid big bang-big crunch algorithm to optimize the sizing of a stand-alone hybrid power system formed by a photovoltaic (PV) generator, a wind turbine (WT), and a battery bank (BB). The simulations demonstrate that this algorithm is able to find an optimal solution when compared to particle swarm optimization (PSO) and discrete harmony search algorithms [11].

The optimization model for a hybrid system proposed by Merei et al. [12] involves three different battery technologies and uses irradiation, wind speed, and air temperature data, all measured in situ. The outcomes confirmed the authors' assumption that using batteries in combination with the renewables is economically and environmentally more efficient.

Applying the strength Pareto evolutionary algorithm to the multiobjective optimization of a stand-alone photovoltaic–wind–diesel system with battery storage minimizes the levelized cost of energy and the equivalent CO_2 life cycle emissions, according to Dufo et al. [13]. Additionally, the results point to the PV generator as the most significant source of electrical energy for these types of systems in Spain and southern Europe.

The sizing method of the hybrid system components based on SDO is also a good practice to find and compare different technical optimization approaches [14]. According to Castañeda et al., a hybrid system may be improved using SDO [15]. As to the results, it can fulfill the energy demands but also store some energy for backup. The simulation of the hybrid system components and the optimization of the total annual cost function using an efficient artificial bee swarm optimization algorithm seem to be a perfect combination for sizing a hybrid energy system, in line with the framework recommended by Maleki et al. [16].

Lau et al. [17] performed a techno-economic feasibility assessment for a hybrid PV–diesel energy system in remote areas. The evaluation reveals the impact of PV penetration and battery storage on energy production, energy cost, diesel generator operational hours, fuel-saving percentage, and CO_2 emissions reduction.

Various studies also compare different optimization tools and algorithms, such as the one performed by Khare et al. [18], indicating that for a PV–wind hybrid system, PSO can find more precise results and has faster convergence than HOMER.

3. System model

The proposed hybrid system takes advantage of Santay Island's natural resources. Wind energy production cannot be efficiently exploited since the island lacks powerful airstreams. Hence, it only combines the water flow of the Guayas River through a hydrokinetic turbine (HKT) with the solar radiation experienced in Ecuador's coastal region through several PV generators.

HOMER gives a 22-year average monthly solar radiation data obtained from the National Aeronautics and Space Administration (NASA). It ranges from a minimum of 2.2 kWh/m^2 per day in December up to a maximum of 6.8 kWh/m^2 per day in June. The annual average radiation is 4.63 kWh/m^2 per day.

According to the Oceanographic Institute of the Ecuador Army, the minimum, maximum, and average water speed for a whole year are 0.31 m/s, 2.26 m/s and 1.39 m/s, respectively.

Although both renewable energy sources present major challenges due to weather unpredictability, their integration improves the techno-economic efficiency of the system and ensures supply reliability.

The accurate battery sizing of the energy storage is crucial to soften the delay of electricity distribution from the generation system to the loads. Despite system effectiveness and ecological impact, an additional diesel generator is considered, since the main system may fail due to internal or external events such as main

generators or BB issues, unforeseen situations, and stages of extremely high demand. Figure 2 displays the configuration of the system.

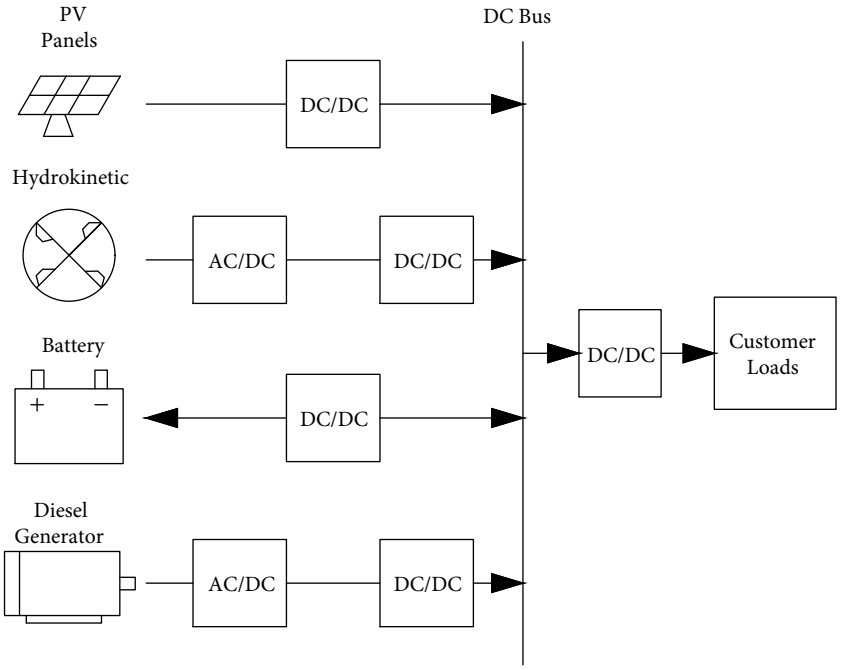

Figure 2. Configuration of the hybrid system.

3.1. Mathematical model of the system components

The mathematical modeling of systems and its components (PV + HKT – Pbat – Pload) is necessary to predict various aspects of the system performance. In addition, for the system to work safely and economically, the model must consider relevant meteorological data and an accurate load assessment [19].

3.2. PV generator

Accurate, meticulous solar radiation prediction is crucial for modeling PV generation. Even though a series of empirical models can predict global solar radiation [20], there currently exists sophisticated software to precisely estimate solar radiation. The software use various meteorological parameters, such as latitude, longitude, and altitude, as well as climatological parameters, such as the duration of the sun, humidity, index of clarity, months, temperature, cloud cover, wind speed, atmospheric pressure, and diffuse radiation [21].

The output power of the PV generator (P_{PV}), measured in kW, represents the PV as a function of the solar radiation incident on the PV array in the current time step (G_T) in kW/m^2, the incident radiation at standard test conditions ($G_{T,STC}$) that is a constant value of 1 kW/m^2, the rated power of the PV panels ($P_{PV,Rated}$), measured in kW, and the scale factor (d_r), which takes into account the reduction of output power in operating conditions of the real world in comparison with the nominal P_{PV} conditions. Eq. (1) mathematically models P_{PV}.

$$P_{PV} = P_{PV,\,Rated} \times d_r \times \left(\frac{G_T}{G_{T,STC}} \right) \tag{1}$$

The PV in question was a Canadian Solar Pro model CS6K-285M (Guelph, ON, Canada). It has a scale factor of 88%, a capacity of 0.285 kW, a lifetime of 25 years, a temperature effect on power of –0.41%/C, and an efficiency of 17.4%.

3.3. Fluvial hydrokinetic generator

This technology is reliable in supplying renewable energy, at low power levels, to remote or isolated areas [22]. Further, its environmental impact is virtually zero, unlike conventional hydroelectric systems [23]. The principle of the HKT operation is very simple: the hydrokinetic system extracts the kinetic energy of water flow without the need for a dam or penstock.

According to Maniaci et al. [24], the energy generated by a hydrokinetic system (E_{HKT}) is a function of the density of water (ρ_W) in kg/m^2, HKT performance coefficient ($C_{p,H}$), combined HKT-generator efficiency (η_{HKT}), HKT area (A) in m^2, water flow velocity (v) in m/s, and time (t) in s. Eq. (2) mathematically expresses E_{HKT}.

$$E_{HKT}=\frac{1}{2}\times\rho_W\times A\times v^3\times C_{p,H}\times\eta_{HKT}\times t \tag{2}$$

Additionally, the block diagram consists of equations based on the open channel velocity profile in accordance with power and logarithmic laws. This law is theoretically sophisticated but its widespread usage is due to its ability to represent vertical velocity profiles more precisely than other similar formulas [25]. In open channel flow, velocity at a certain point above the river bed is considered as a form of power function using depth ratio. It takes into account the stream-wise time-mean velocity (u), upward bed-normal distance above datum (y), velocity at point a where it is vertically deviated from river bottom (u_a), and power law exponent ($^1/_m$). Therefore, the power law can be expressed as in Eq. (3).

$$\frac{u}{u_a}=\left(\frac{y}{a}\right)^{1/m} \tag{3}$$

The block diagram can be finally found once the river flow velocity and the HKT power curve are known. The commercial fluvial turbine used in this project is a 5 kW Smart Monofloat (Smart Hydro Power; Feldafing, Germany), which ranges from 0.25 kW to 5 kW. It has 3 rotor blades with a diameter of 1000 mm, capable of generating a rotational speed of 90 to 230 rpm. This subsystem includes a block called "water density ratio function," as recommended by the manufacturer, to replicate river water conditions in the best way; hence, it avoids inconsistent variations in simulation results. Figure 3 shows the final block diagram for the simulated HKT.

3.4. Battery bank

The output of the renewable power supply (PV + HKT) and the users' demand per hour determine the energy load, or unload, of the batteries. With this in mind, the BB is modeled using a generic 1 kWh lead-acid battery [26], which has a nominal voltage of 12 V, a maximum capacity of 83.4 Ah, a capacity ratio of 0.403, a rate constant of 0.827 1/h, and a maximum charge current of 16.7 A.

Depending on the energy produced from renewable resources and the load power demand, the state of

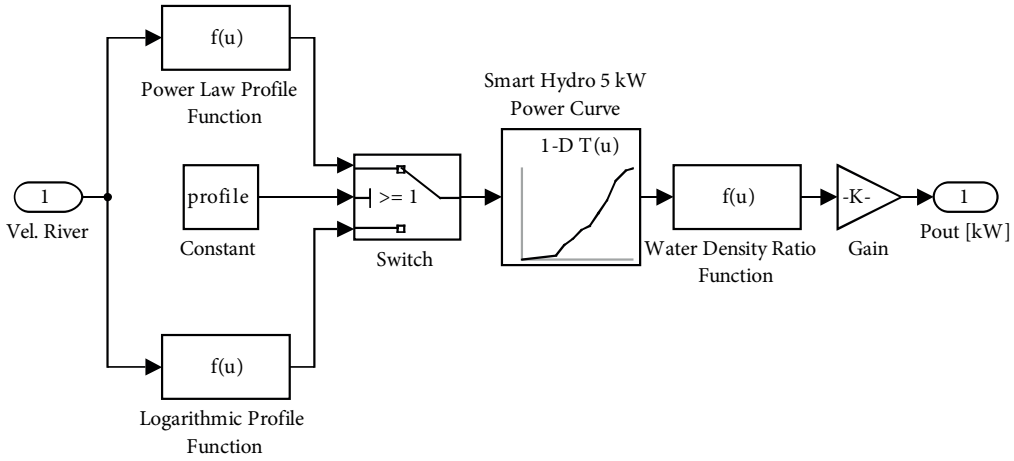

Figure 3. Block diagram of a river HKT using Simulink.

charge of the battery, for the charging and discharging modes, can be calculated from Eqs. (4) and (5) [27].

$$SOC\,(t) = SOC\,(t-1) + \frac{E_{bat}\,(t) \times \eta_{cbat}}{P_{bat}} \times 100 \tag{4}$$

$$SOC\,(t) = SOC\,(t-1) + \frac{E_{bat}\,(t) \times \eta_{dbat}}{P_{bat}} \times 100, \tag{5}$$

where $SOC\,(t)$ is the state of charge at time t, E_{bat} is the power exchange during the time step Δt, P_{bat} is the nominal capacity of the battery, and η_{cbat} and η_{dbat} are the battery charge and discharge efficiency, respectively.

3.5. Diesel generator

Habitually, hybrid systems incorporate diesel generators (DGs) for security purposes, i.e. just in cases of adverse conditions that might interrupt the correct supply of renewable energy. The strategy for energy delivery and the status of the battery are the main determinants that turn on or off the DG. The model proposed reflects the following power monitoring strategy: when the objective function PV + HKT – Pload – Pbat yields values below the lower hysteresis limit of the system, the DG switches on, which produces enough electricity to fulfill the load demand and charges the BB [28]. In contrast, when the objective function exceeds the upper hysteresis limit, the system switches the DG off and puts the renewable energy generator to work [29]. This approach switches the DG on only when necessary, but always under economic and environmental efficiency.

The block diagram, designed in Simulink, uses a simple first-order model that gives a satisfactory approach of the fuel consumption rate (fuel rack position) as a function of speed and mechanical power at the output of the engine [30]. The input data for the diesel generator model was set up as follows: power of 10 kW, a cylinder bore diameter of 77 mm, a piston stroke of 81 mm, and a rate of 1800 rpm.

3.6. Energy management

While the system model plays an important role in long-term sizing, system energy management does not. For this reason, the energy management model used is simple. As shown in Figure 4, the power supplied by renewable sources (P_Renov) is calculated from the input time series of velocity river (H_River) and solar

radiation (H_Solar). In each calculation step, the net power PR_PC is obtained as the difference of the renewable power and the power requested by the load. PR_PC is then delivered to the battery system. If it is positive, the battery is charged; if it is negative, the battery is discharged. In this last situation, the DG is used to supply the deficiency only if the battery cannot cover the lack of power.

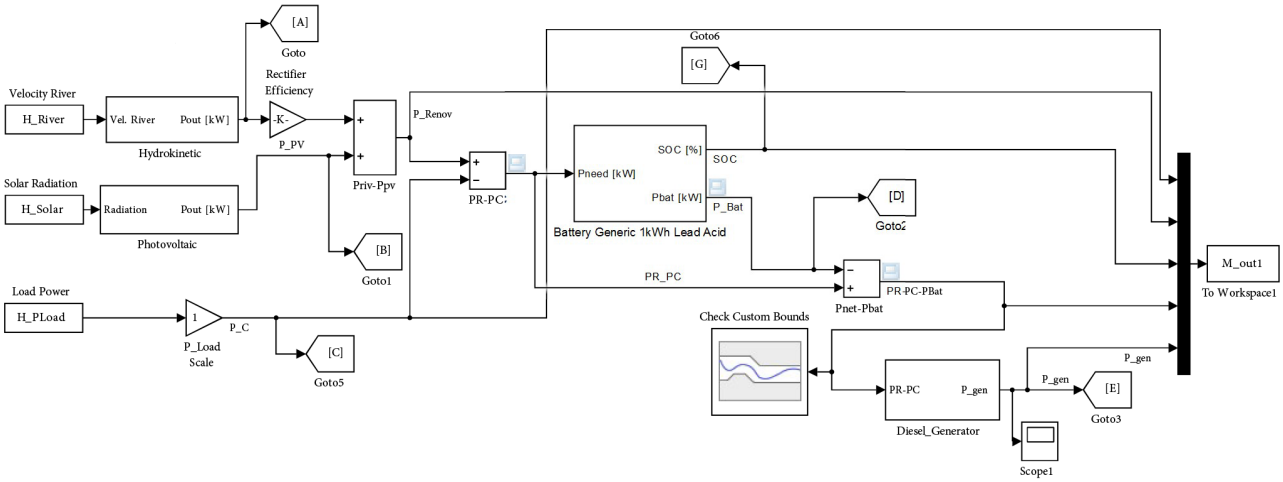

Figure 4. Block diagram of the hybrid system.

3.7. The hybrid system

To meet the objectives, this project uses the response optimization option of SDO for parameter tuning. First, the selection of the tuning parameters (the model parameters to be optimized) is carried out, whereas the rest remain as defined parameters. In this context, the PV, HKT and number of batteries for the BB are the tuning parameters, while the DG rated power is a defined parameter. For the optimization process, the initial, minimum, and maximum values of each tuning parameter need to be set. The initial values, or seeds, and the parameters' variation range can be found through the mathematical model equations of the system components. Therefore, the accuracy of these values, as well as the precision of mathematical models, conveys a positive optimization process.

Secondly, the model signal has to be determined, taking into account the fitting values of the tuning parameters to prevent it from exceeding the limits. The signal selected in the optimization process is the accumulated power at the battery PV + HKT – Pbat – Pload.

For the proposed sizing, once Pbat reaches a value between 0 kW and –9 kW, the system switches the DG on. The set value corresponds to the DG power; the input signal satisfies the specified limits. The limits are set by indicating by pairs of values ??the time and the amplitude of each section.

Finally, the optimization and search methods can be chosen through the optimization options label. There are three types of optimization methods: gradient descent, pattern search, and simplex search. After testing several cases, pattern search was selected because it permits finding appropriate values for the tuning parameters. Additionally, this study considers three out of the five algorithms available for pattern search because of the optimization level found after various tests. Latin hypercube, genetic algorithm and Nelder–Mead yielded the most suitable results when applied to the system simulation.

Nonetheless, in order to control the optimization process, four parameters must be understood: parameter tolerance, which ends the optimization process when successive parameters values change less than this indicator;

constraint tolerance, which represents the maximum value by which the constraints may be violated but still allow a successful convergence; function tolerance, which ends the optimization process when successive function values are less than this indicator and was not used since it is only useful for simplex search method; and maximum iterations, which states the maximum number of iterations the optimization process may run.

Once all these processes are performed, the SDO automatically converts the requirements specified in task two into a constrained optimization problem. Thus, it solves the problem utilizing the optimization method and algorithm chosen in task three.

Figure 4 shows the simulated model, where all the electricity generators, i.e. PV, HKT, BB, and DG, are connected to a common DC bus through power converters for energy management. The application of SDO optimization techniques to the system sizing chosen validates the reliability of the system [8].

Figure 5 displays the estimation of electricity consumption per hour from the characteristic curve of the Ecuadorians' residential consumption [31]. Based on the numerical data of this curve extracted by the software Engauge Digitizer, the minimum value is 3.1 kW, the maximum 5.6 kW, and the average 4.18 kW. A time series based on this profile is used as load input H_Pload of the hybrid systems.

Figure 6 shows real weather data for solar irradiance at 1-h intervals over 1 year. These data is obtained through the HOMER software from NASA. The PV generator uses this data as input H_Solar to simulate and optimize the system.

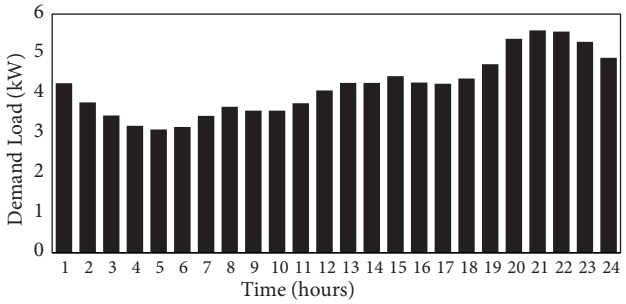

Figure 5. Residential consumption per hour.

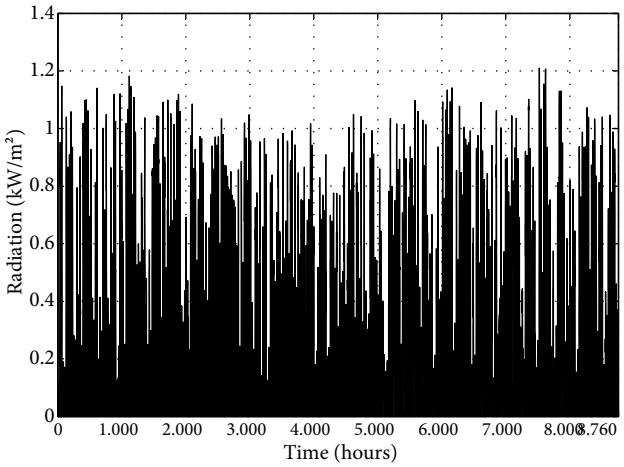

Figure 6. Solar radiation.

A time series of the river flow speed based on the data provided from the Oceanographic Institute of the Ecuador Navy is used as input H_River of the HKT.

4. Results analysis and discussion

The proposed algorithm assumes that Santay Island lacks access to the electricity grid due to geography issues. Table 1 presents the outcomes of the technical sizing following the SDO pattern search method, adjusting parameters via the three methods this tool offers: Latin hypercube, genetic algorithm, and Nelder–Mead. To validate the optimal sizing, the results are compared to those obtained through HOMER.

Furthermore, Table 2 displays the results for the hybrid system components considering the same optimization methods in a 1-year period.

Table 1. Outcomes of optimized subsystem sizing via SDO and HOMER.

	Simulink design optimization			HOMER
	Genetic algorithm	Latin hypercube	Nelder–Mead	
HKT power (kW)	10.05	10.10	10.00	10
Diesel generator (kW)	10	10	10	10
PV power (kW)	10.20	10.16	10.10	11
Battery capacity (kWh)	399.84	400.24	391.55	160.13

Table 2. Outcomes of optimized sizing per year via SDO and HOMER for each subsystem and the complete hybrid system.

	Simulink design optimization			HOMER
	Genetic algorithm	Latin hypercube	Nelder–Mead	
HKT energy (kWh/year)	20,230	20,330	20,130	20,130
Generation diesel (kWh/year)	5688	5668	5870	5335
PV power energy (kWh/year)	13,630	13,580	13,500	14,700
Batteries energy (kWh/year)	–128.8	–119.4	–166.1	–88.7
Average battery SOC (%)	53.74	54.07	52.15	57.86
Minimum battery SOC (%)	38.47	38.55	38.70	35.92

Figure 7 shows the DG on/off, operation, and its maximum power (kW) required to supply the demand. Using the Latin hypercube algorithm, the energy contributed is 5668 kWh/year. As shown in Table 2, after using the three SDO algorithms, the battery reaches a minimum SOC of 38.4% using genetic algorithm, 38.5% using Latin hypercube, and 38.7% using Nelder–Mead, whereas HOMER achieves a minimum of 35.9%. Consequently, SDO accomplishes a lower depth of discharge but a longer battery lifetime.

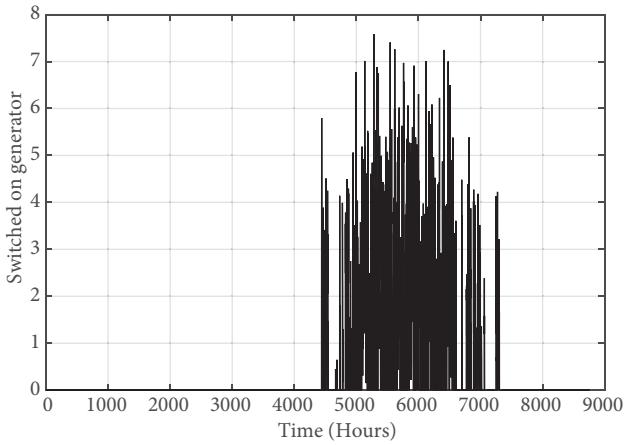

Figure 7. DG on using method Latin hypercube.

5. Conclusion

The implementation of autonomous hybrid systems for the generation of renewable energy in isolated areas or national parks tends to be economically and environmentally more effective and so much more reliable than systems exploiting only one renewable resource.

This hybrid system demonstrates that safe, clean energy can be supplied, despite low meteorological predictability, to the inhabitants of a protected wildlife zone.

The proposed system would take into consideration the local environmental resources through a technically optimized sizing that allows the best possible match between supply and demand. Moreover, this system uses ecosystem-friendly equipment and reduces the duty time of DGs.

The results of the SDO tool indicate a greater storage capacity in the batteries when compared to HOMER. Furthermore, the Latin hypercube algorithm gives better performance with a limited use of the diesel generator than the other algorithms.

The next step is to achieve a new method of economic technical feasibility for the hybrid system with generators of renewable origin, eliminating the use of the diesel generator.

Nomenclature

ABSO	Artificial bee swarm optimization algorithm
BB	Battery bank
$C_{p,H}$	HKT performance coefficient
ICE	Internal combustion engines
CO_2	Carbon dioxide (kg/year)
DG	Diesel generator (kW)
DHS	Discrete harmony search
E_{bat}	Power exchange during the time step (kWh)
E_{HKT}	Energy generated by the HKT (kWh)
G_T	Solar radiation incident (kW/m^2)
$G_{T,STC}$	Incident radiation at standard test condition (1 kW/m^2)
HBB-BC	Hybrid big bang-big crunch algorithm
HKT	hydrokinetic turbines
HRE	Hybrid renewable energy
LCE	Life cycle emissions
LCOE	Levelized cost of energy ($/ kWh)
Pbat	Power battery (kW)
P_{bat}	Nominal capacity of the battery (kWh)
Pload	Power load (kW)
P_{PV}	Power PV nominal (kW)
$P_{PV,Rated}$	Rated power of the PV (kW)
PSO	Particle swarm optimization
PV	Photovoltaic panels
SDO	Simulink design optimization
SOC	State of charge (%)
u	Streamwise time-mean velocity
u_a	Velocity at point a where it is vertically deviated from river bottom
y	Upward bed-normal distance

v	Water flow velocity (m/s)
ρ_W	Density of water (kg/m^3)
η_{HKT}	HKT-generator efficiency
η_{cbat}	Battery charge efficiency (%)
η_{dbat}	Battery discharge efficiency (%)
$^1/_m$	Power law exponent

References

[1] Kaygusuz K. Energy for sustainable development: key issues and challenges. Energ Source Part B Econ Planning Policy 2007; 2: 73-83.

[2] Selim MYE, Elfeky SMS. Effects of diesel/water emulsion on heat flow and thermal loading in a precombustion chamber diesel engine. Appl Therm Eng 2001; 21: 1565-1582.

[3] Koko SP, Kusakana K, Vermaak HJ. Micro-hydrokinetic river system modelling and analysis as compared to wind system for remote rural electrification. Electr Pow Syst Res 2015; 126: 38-44.

[4] Vermaak HJ, Kusakana K, Koko SP. Status of micro-hydrokinetic river technology in rural applications: a review of literature. Renew Sust Energ Rev 2014; 29: 625-633.

[5] Luna-Rubio R, Trejo-Perea M, Vargas-Vázquez D, Ríos-Moreno GJ. Optimal sizing of renewable hybrids energy systems: a review of methodologies. Sol Energy 2012; 86: 1077-1088.

[6] Montoya Ramírez RD, Cuervo FI, Monsalve CA. Technical and financial valuation of hydrokinetic power in the discharge channels of large hydropower plants in Colombia: a case study. Renew Energ 2016; 99: 136-147.

[7] Nema P, Nema RK, Rangnekar S. A current and future state of art development of hybrid energy system using wind and PV-solar: a review. Renew Sust Energ Rev 2009; 13: 2096-2103.

[8] Cano A, Jurado F, Sánchez H, Fernández LM, Castañeda M. Optimal sizing of stand-alone hybrid systems based on PV/WT/FC by using several methodologies. J Energy Inst 2014; 87: 330-340.

[9] Bahramara S, Moghaddam MP, Haghifam MR. Optimal planning of hybrid renewable energy systems using HOMER: a review. Renew Sust Energ Rev 2016; 62: 609-620.

[10] Lata-García J, Reyes-Lopez C, Jurado F. Attaining the energy sustainability: analysis of the Ecuadorian strategy. Probl Ekorozw 2018; 13: 21-29.

[11] Ahmadi S, Abdi S. Application of the Hybrid Big Bang–Big Crunch algorithm for optimal sizing of a stand-alone hybrid PV/wind/battery system. Sol Energy 2016; 134: 366-374.

[12] Merei G, Berger C, Sauer DU. Optimization of an off-grid hybrid PV–wind–diesel system with different battery technologies using genetic algorithm. Sol Energy 2013; 97: 460-473.

[13] Dufo-López R, Bernal-Agustin J, Yusta-Loyo JM. Multi-objective optimization minimizing cost and life cycle emissions of stand-alone PV–wind–diesel systems with batteries storage. Appl Energ 2011; 88: 4033-4041.

[14] Lata-Garcia J, Reyes-Lopez J, Jurado F, Fernandez-Ramirez L, Sanchez H. Sizing optimization of a small hydro/photovoltaic hybrid system for electricity generation in Santay Island, Ecuador by two methods. In: IEEE 2017 Electrical, Electronics Engineering, Information and Communication Technologies Conference; 18–20 October 2017; Pucon, Chile: IEEE. pp 1-6.

[15] Castañeda M, Cano A, Jurado F, Sánchez H, Fernández LM. Sizing optimization, dynamic modeling and energy management strategies of a stand-alone PV/hydrogen/battery-based hybrid system. Int J Hydrogen Energ 2013; 38: 3830-3845.

[16] Maleki A, Askarzadeh A. Artificial bee swarm optimization for optimum sizing of a stand-alone PV/WT/FC hybrid system considering LPSP concept. Sol Energy 2014; 107: 227-235.

[17] Lau KY, Yousof MF, Arshad SN, Anwari M, Yatim AH. Performance analysis of hybrid photovoltaic/diesel energy system under Malaysian conditions. Energy 2010; 35: 3245-3255.

[18] Khare V, Nema S, Baredar P. Optimisation of the hybrid renewable energy system by HOMER, PSO and CPSO for the study area. Int J Sustain Energy 2017; 36: 326-343.

[19] Khare V, Nema S, Baredar P. Solar–wind hybrid renewable energy system: a review. Renew Sust Energ Rev 2016; 58: 23-33.

[20] Quej VH, Almorox J, Ibrakhimov M, Saito L. Estimating daily global solar radiation by day of the year in six cities located in the Yucatán Peninsula, Mexico. J Clean Prod 2017; 141: 75-82.

[21] Mohanty S, Patra PK, Sahoo SS. Prediction and application of solar radiation with soft computing over traditional and conventional approach – a comprehensive review. Renew Sust Energ Rev 2016; 56: 778-796.

[22] Kusakana K. Techno-economic analysis of off-grid hydrokinetic-based hybrid energy systems for onshore/remote area in South Africa. Energy 2014; 68: 947-957.

[23] Yuce MI, Muratoglu A. Hydrokinetic energy conversion systems: a technology status review. Renew Sust Energ Rev 2015; 43: 72-82.

[24] Maniaci DC, Li Y. Investigating the influence of the added mass effect to marine hydrokinetic horizontal-axis turbines using a General Dynamic Wake wind turbine code. In: IEEE 2011 Oceans; 19–22 September 2011; Waikoloa, HI, USA, pp. 1-6.

[25] Lee HE, Lee C, Kim YJ, Kim JS, Kim W. Power law exponents for vertical velocity distributions in natural rivers. Engineering 2013; 5: 933-942.

[26] Manwell JF, McGowan JG. Lead acid battery storage model for hybrid energy systems. Sol Energy 1993; 50: 399-405.

[27] Mehrabankhomartash M, Rayati M, Sheikhi A, Ranjbar AM. Practical battery size optimization of a PV system by considering individual customer damage function. Renew Sust Energ Rev 2017; 67: 36-50.

[28] Manwell JF, Stein WA, Rogers A, McGowan JG. An investigation of variable speed operation of diesel generators in hybrid energy systems. Renew Energ 1992; 2: 563-571.

[29] Tazvinga H, Zhu B, Xia X. Optimal power flow management for distributed energy resources with batteries. Energ Convers Manage 2015; 102: 104-110.

[30] Roy S, Malik OP, Hope GS. Adaptive control of speed and equivalence ratio dynamics of a diesel driven power-plant. IEEE T Energy Conver 1993; 8: 13-19.

[31] Plan Maestro de Electrificación 2013-2022. Residential load curve, Guayaquil Electric 2017; 2: 42.